Journal of the European Ceramic Society **19** (1999) 2421–2426

PII: S0955-2219(99)00112-0
0955-2219/99/$ - see front matter

Oxide Composites of Al_2O_3 and $LaPO_4$

J. B. Davis,* D. B. Marshall and P. E. D. Morgan

Rockwell Science Center, 1049 Camino Dos Rios, Thousand Oaks, CA 91360, USA

Abstract

Some properties of oxide composites based on Al_2O_3 and $LaPO_4$ (La-monazite) are examined. A composite consisting of woven Al_2O_3 fibers with a porous matrix of Al_2O_3 and $LaPO_4$ is shown to be damage tolerant and notch insensitive. The feasibility of achieving fiber sliding and pullout in a composite with a fully dense matrix is investigated using a small hot-pressed composite of sapphire fibers and $LaPO_4$ matrix. © *1999 Elsevier Science Ltd. All rights reserved.*

Keywords: $LaPO_4$, composites, fibres, mechanical properties, Al_2O_3.

1 Introduction

Damage-tolerant, nonlinear behavior in ceramic composites requires weak surfaces or phases that decouple fracture processes in the matrix and the fiber reinforcements. This can be achieved in composites with a weak interphase separating strong fibers from a strong matrix, such as in glass-matrix/SiC-fiber composites with a weak carbon interphase.[1–3] It can also be achieved in composites consisting of strong fibers in a porous, weak matrix, such as in carbon–matrix composites.[4,5] Until fairly recently, all ceramic composites relied on either carbon or BN for the weak phase. As a result, they suffered from limited oxidation resistance.

During the past 5 years, several analogous oxide systems have been identified, with potential for long-term stability in oxidizing environments. Composites with weak porous matrices of SiO_2/Al_2O_3,[6] Al_2O_3,[7] Al_2O_3/mullite,[8,9] and $AlPO_4$[10] have been reported with room temperature mechanical properties very similar to carbon–carbon composites. These oxide composites were fabricated by infiltration of slurries into preforms of woven fibers (small-diameter, polycrystalline alumina or mullite fibers) followed by sintering. In the absence of a separate weak interphase between the fibers and matrix, the porous matrix bonds strongly to the fibers. However, because of the low elastic stiffness and fracture toughness resulting from the porosity, cracks do not readily pass from the matrix to the fibers, and tensile loading causes extensive damage in the matrix before failure of the fibers. Failure ultimately involves pullout of fibers, mainly in tows, and the fracture strength is relatively insensitive to the presence of stress concentrators such as notches and holes.[9] The high temperature limitations of such composites are expected to come from several sources: microstructural stability of fine grained fibers, coarsening of the matrix, and interdiffusion of the matrix and fibers.

In fully dense systems, two classes of oxides that allow debonding have recently been identified. One relies on layered crystal structures such as micas,[11] β-aluminas,[12] magnetoplumbites[12,13] and perovskites,[14] with intrinsically weak cleavage planes. The other is a group of refractory mixed oxides (rare-earth orthophosphates with the monazite[15–18] or xenotime[19] structures, and several tungstates[20] and vanadates[21]), which have been shown to form weak interfaces with other oxides such as Al_2O_3, YAG, ZrO_2, and mullite. In the case of La-monazite ($LaPO_4$), long-term stability with sapphire fibers has been demonstrated at 1600°C,[18] thus indicating the prospect of fabricating dense-matrix composites with better stability than the porous matrix systems presently available. However, most studies of these systems have involved model specimen configurations designed to assess interfacial debonding. With the exception of some multilayered composites,[17] fully dense composites have not been formed, mainly because of the difficulty of processing such composites without degrading the oxide fibers that are presently available.

In this paper we present some properties of an oxide composite that combines a porous matrix and a weak fiber–matrix interface to give enhanced nonlinear behavior and potentially improved stability at high temperatures. The composite consists of polycrystalline Al_2O_3 fibers in a porous, two-phase matrix of $LaPO_4$ and Al_2O_3. We also report some preliminary experiments to test the ability of $LaPO_4$ to facilitate fiber debonding and pullout in fully dense systems.

*To whom correspondance should be addressed.

2 Experiments

A porous matrix composite was fabricated by infiltrating woven fabric of polycrystalline alumina fibers (3M company, Nextel 610, 8-harness satin weave) with a slurry of $Al_2O_3/LaPO_4$. The slurry contained dispersed α-alumina powder (Sumitomo, AKP50) and solution precursor for $LaPO_4$. Individual layers of fabric, 15×15 cm^2, were infiltrated, stacked (10 layers), dried while vacuum bagging and warm pressing, then sintered at 1100°C in air for 1 h. The resulting composite plate was ~2 mm thickness. Double-edge-notched tensile test specimens, with dimensions $\sim 15 \times 1$ cm aligned parallel to the weave direction, were cut from the plate using a diamond saw (Fig. 1). The saw cuts that formed the notches were of ~150 μm width. The specimens were loaded in tension using wedge grips and tabs glued to the ends. The gauge section extension was measured using a clip gauge attached 12·5 mm above and below the mid plane, which contained the notches.

A composite with a fully dense $LaPO_4$ matrix and sapphire fiber reinforcement was fabricated by hot pressing. Since the sole purpose of this composite was to test whether debonding and fiber pullout occur in this system under tensile loading parallel to the fibers, the simplest possible fabrication route, making use of available hot pressing facilities, was used. Sapphire fibers were chosen to allow hot pressing at sufficiently high temperature to densify the matrix (1400°C) without damaging the fibers (polycrystalline fibers would degrade at this temperature). Approximately 200 fibers of length 40 mm were coated individually with a thick layer of rhabdophane (hydrated $LaPO_4$) powder and stacked together along a diameter of a 50 mm cylindrical graphite die. The remainder of the die was filled with Al_2O_3 powder to prevent direct contact between the graphite die and the $LaPO_4$. The compact was hot pressed at 1400°C for 1 h, to form an alumina disk with a small embedded sapphire/$LaPO_4$ composite, of cross-section dimensions $\sim 2 \times 2$ mm, along its diameter.

The test specimen shown schematically in Fig. 2 was cut from the hot pressed disc and loaded in four-point bending with the embedded composite in tension. The hole drilled adjacent to the embedded composite served to reduce the gradient of tensile bending stress across the composite and to allow cracking of the ligament of material between the hole and the edge of the specimen without fracturing the entire beam.

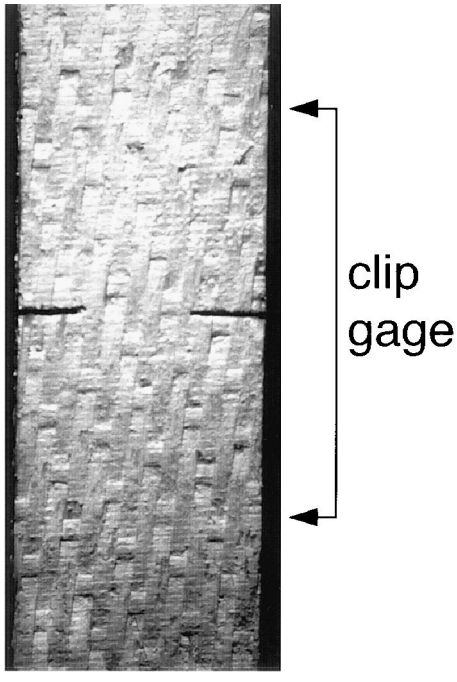

Fig. 1. Double-edge-notched tensile test specimen of composite consisting of woven Al_2O_3 fibers and porous Al_2O_3–$LaPO_4$ matrix.

3 Results

3.1 Porous $Al_2O_3/LaPO_4$ matrix composites

The microstructure of the $Al_2O_3/LaPO_4$ matrix composite is shown in the scanning electron microscope (SEM) image of Fig. 3. The matrix consists of a two-phase mixture of Al_2O_3 and $LaPO_4$ grains, both with dimensions smaller than approximately 0·5 μm, with fine-scale porosity between the grains. The alumina grains in the matrix are always separated from the fibers by a thin layer of $LaPO_4$. The composites consisted of approximately 40 vol% of fibers (20% in each of the 0 and 90° orientations), 40 vol% matrix (Al_2O_3 and $LaPO_4$ in the ratio approximately 2:1) and 20 vol% porosity (as estimated from weight measurements).

The tensile response of a test specimen with notch depth greater than half of the test section ($a/w = 0{\cdot}54$) is shown in Fig. 4. The net section stress during testing (load divided by the remaining cross-sectional area between the ends of the notches) is plotted as a function of the extension measured from the clip gauge. Also shown along the top border is the average strain calculated from the

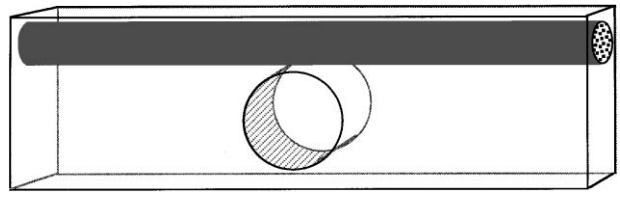

Fig. 2. Test specimen (Al_2O_3) with embedded composite of sapphire fibers and $LaPO_4$ matrix.

extension measurements; however, the strain is very nonuniform within the gauge area. The stress–strain curve shows substantial nonlinearity in the loading portion and continuously decreasing load beyond the peak. Test specimens without notches showed similar stress–strain curves, with strengths, in the range 200 to 220 MPa.

The nonlinear response is associated with extensive pullout of fibers, as seen from the separated ends of the test specimen in Fig. 5. Failure of the specimen occurred by separation of the matrix along an approximately planar section between the ends of the two notches and pullout of individual fibers over lengths up to ~1 cm from both sides of the fracture plane. Small but finite loads were supported by these bridging fibers at crack opening displacements of several mm. Examples of intact specimens loaded beyond the peak in the stress–strain curve are shown in Fig. 6: at a crack opening of ~1 mm in Fig. 6(a), (showing bridging fibers) and at a crack opening of ~3 mm in Fig. 6(b) (*in-situ* micrograph with net section stress 8 MPa).

3.2 Fully dense $LaPO_4$-matrix composite

The microstructure of the hot pressed $LaPO_4$-matrix composite is shown in the polished cross-section of Fig. 7. The matrix contains a few isolated pores, but is mostly fully dense $LaPO_4$. There is no apparent degradation of the sapphire fibers or reaction with the matrix.

Micrographs of the specimen depicted in Fig. 2 after loading to failure are shown in Fig. 8. Pullout of the sapphire fibers occurred over lengths of several mm, with most fibers pulling out from one side of the fracture surface. Although extensive cracking occurred in the $LaPO_4$ matrix, and pieces of the matrix pulled out with the fibers as in Fig. 8(a), higher magnification micrographs such as Fig. 8(b) show that debonding and sliding occurred at the fiber–matrix interface [scratch marks due to fiber sliding can be seen in the $LaPO_4$ matrix in Fig. 8(b), in the hole left behind after pulling out the fiber].

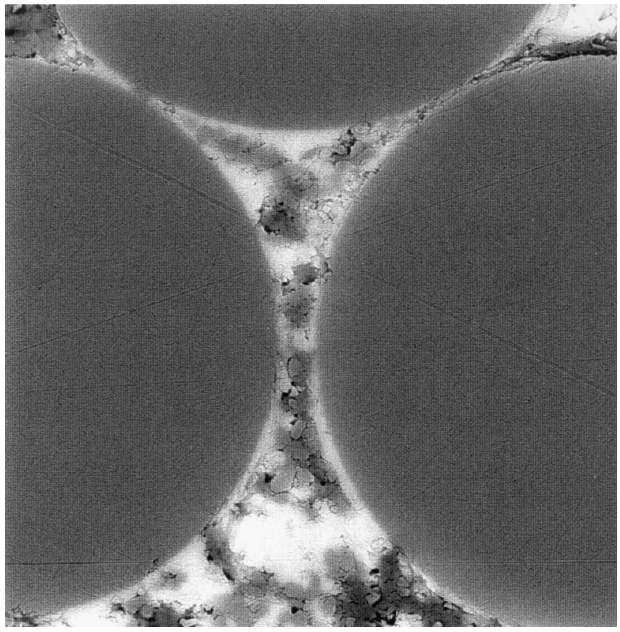

Fig. 3. Microstructure of composite from Fig. 1 (secondary electron image).

4 Discussion

Under tensile loading parallel to the 0 or 90° weave direction, the $Al_2O_3/LaPO_4$ matrix composite shows nonlinear stress–strain response, with the nonlinear component of strain at the peak load being several times the linear elastic strain extrapolated from low loads. Failure is non-catastrophic, with fiber pullout over distances of ~1 cm. Strengths, in the range 200–250 MPa, are unaffected by the presence of severe notches. These characteristics differ from the responses reported

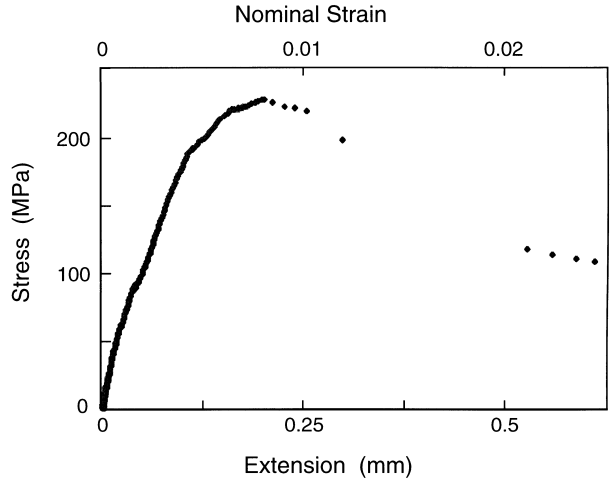

Fig. 4. Tensile test results from composite of Fig. 1.

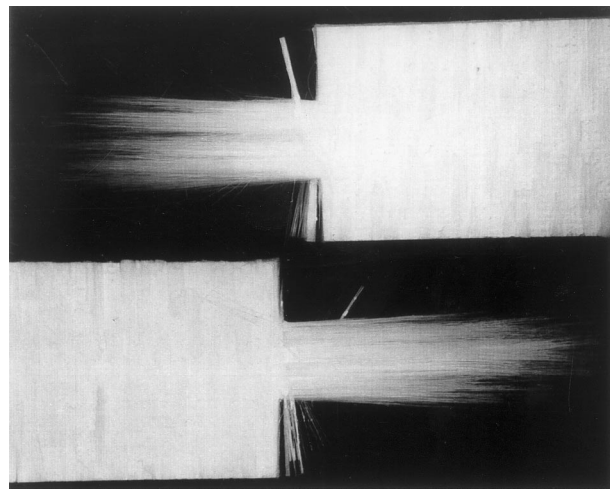

Fig. 5. Separated test specimen from test in Fig. 4.

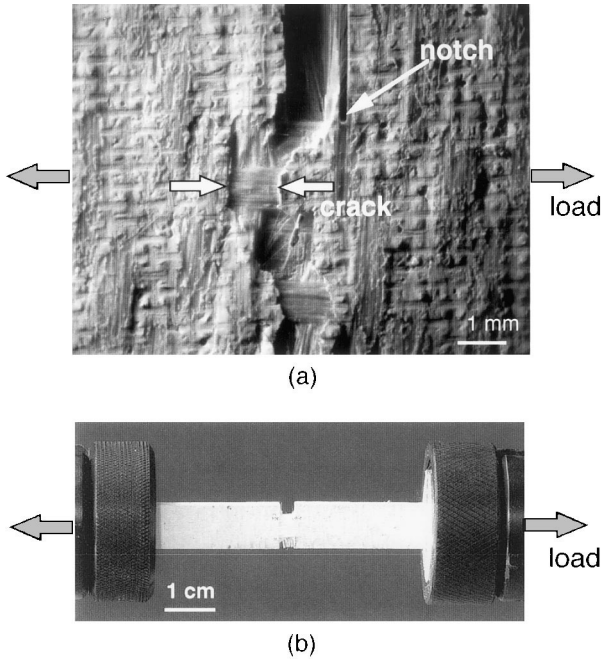

Fig. 6. (a) Bridging fiber tows in test specimen loaded as in Fig. 4, interrupted before complete separation. (b) *In-situ* optical micrograph from test as in Fig. 4 at net section stress of 8 MPa.

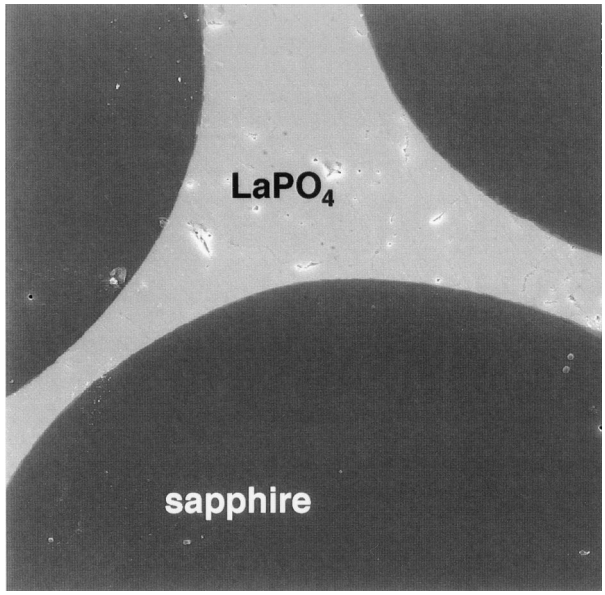

Fig. 7. Cross-section of hot-pressed $LaPO_4$-matrix composite (secondary electron image).

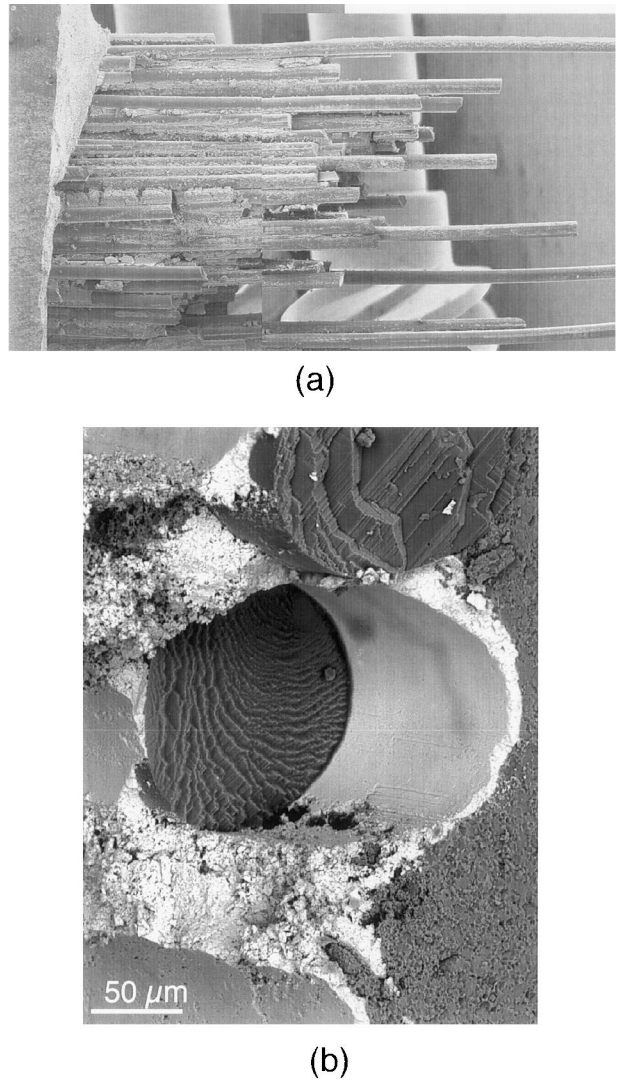

Fig. 8. (a) Fractured test piece of $LaPO_4$ matrix composite. (b) Higher magnification of region of fracture surface from same specimen as (a). Dark circular area is fracture surface of sapphire fiber. Smooth light region is $LaPO_4$ coating in cylindrical hole (going into page from right to left) remaining after pull-out of the other half of the fractured fiber.

for other porous matrix composites in systems where strong local bonding between matrix and fibers would be expected (SiO_2/Al_2O_3,[6] Al_2O_3/mullite,[8,9] $AlPO_4$[10]). The strengths of such composites under loading parallel to the 0 or 90° directions have been reported in the same range, while notch-insensitivity along with nonlinear stress-strain response and noncatastrophic failure have been reported under flexural loading and under tensile loading in a direction at 45° to the 0/90 weave direction.[9] However, the large nonlinear response has not been observed in tensile loading parallel to the 0 or 90° weave directions. In this case, the composites may show a very small nonlinearity before the peak load (nonlinear component of strain less than 10% of the total strain) and a jagged fracture surface associated with some pullout of fiber tows. However, failure is catastrophic and the extensive pullout of individual fibers, such as in Fig. 5, is not observed. Therefore, it is evident that, while the porous nature of the matrix in the $Al_2O_3/LaPO_4$ composite most likely contributes to the nonlinear response, the presence of the weakly bonded $LaPO_4$ phase at the fiber–matrix interface greatly enhances the damage-tolerant behavior of the composite.

Although porous-matrix composites may be adequate for many applications, certain uses bene-

fit from, or require a fully dense matrix (e.g., extremely corrosive environments, need for hermetic seal). Previous studies of $LaPO_4/Al_2O_3$ interfaces have demonstrated that debonding occurs in a variety of cracking configurations in fully dense systems.[15–18] However, damage-tolerant behavior requires sliding and pullout of fibers in addition to debonding. Fiber sliding after debonding would be expected to be more difficult in fully dense systems than in composites with porous matrices, because the higher stiffness of the matrix would be less accommodating for the misfit caused by the sliding motion of any irregularities at the interface.[22]

Fiber sliding was demonstrated previously in pushout experiments involving isolated sapphire fibers with $LaPO_4$ coatings in a fully dense Al_2O_3 matrix.[15] The interface in these experiments contained irregularities in the form of grain boundary grooves and cusps with height ~50 nm. Sliding occurred without permanent deformation, implying that the misfitting asperities were accommodated by elastic strains during sliding. The $LaPO_4$-matrix composite examined in the present study was prepared using the same starting materials and nominally identical processing conditions as the composite used in the previous pushout experiments.[15] The results in Figs. 7 and 8 demonstrate the feasibility of achieving fiber *pullout* in fully dense systems.

The development of oxide composites with fully dense matrices is presently limited by our ability to densify the matrix under conditions that do not degrade the fibers. Processing temperatures for composites containing polycrystalline Al_2O_3 and mullite fibers are limited to ~1200–1300°C (lower if pressure is used to aid densification). Such composites require development of either higher temperature fibers (e.g. eutectic or single crystal fibers) or methods, currently being examined, for promoting densification of the matrix at lower temperatures.

5 Conclusions

An oxide composite consisting of woven Al_2O_3 fibers and a porous matrix of Al_2O_3 and $LaPO_4$ was found to exhibit much greater nonlinear response and notch insensitivity than other porous matrix composites. The enhanced properties were attributed to weak bonding between the fibers and the $LaPO_4$ phase, which allowed extensive fiber pullout.

The feasibility of achieving fiber pullout in fully dense Al_2O_3–$LaPO_4$ composites was demonstrated using a hot pressed composite with sapphire fibers.

Acknowledgements

Funding for this work was provided by the U.S. Air Force Office of Scientific Research under contract F49620-96-C-0026 monitored by Dr. A. Pechenik (work on fully dense matrix composites) and the U.S. Office of Naval Research under contract N00014-95-C-0057 monitored by Dr. S. Fishman (work on porous matrix composite).

References

1. Prewo, K. M. and Brennan, J. J., High strength silicon carbon fiber reinforced glass matrix composites. *J. Mater. Sci.*, 1980, **15**(2), 463–468.
2. Brennan, J. J. and Prewo, K. M., Silicon carbide fiber reinforced glass–ceramic matrix composites exhibiting high strength and toughness. *J. Mater. Sci.*, 1982, **17**(8), 2371–2383.
3. Sun, E. Y., Nutt, S. R. and Brennan, J. J., Fiber coatings for SiC-fiber-reinforced BMAS glass–ceramic composites. *J. Am. Ceram. Soc.*, 1997, **80**(1), 264.
4. Turner, K. R., Speck, J. S. and Evans, A. G., Mechanisms of deformation and failure in carbon–matrix composites subject to tensile and shear loading. *J. Am. Ceram. Soc.*, 1995, **78**(7), 1841–1848.
5. Buckley, J. D., Carbon–carbon, an overview. *Am. Ceram. Soc. Bull.*, 1988, **67**(2), 364–368.
6. Harrison, M. G., Millard, M. L. and Szweda, A., Fiber reinforced ceramic matrix composite member and method for making. U.S. Patent No. 5 306 554; UK Patent No. 2 230 259 (1994).
7. Tu, W. C., Lange, F. F. and Evans, A. G., Concept for a damage-tolerant ceramic composite with 'strong' interfaces. *J. Am. Ceram. Soc.*, 1996, **79**(2), 417–424.
8. Levi, C. G., Yang, J. Y., Dalgleish, B. J., Zok, F. W. and Evans, A. G., Processing and performance of an all-oxide ceramic composite. *J. Am. Ceram. Soc.*, 1998, **81**(8), 2077–2086.
9. Lange, F. F., Tu, W.-C. and Evans, A. G., Processing of damage-tolerant, oxidation-resistant ceramic-matrix composites by a precursor infiltration and pyrolysis method. *Mater. Sci. Eng.*, 1995, **A195**, 145–150.
10. Keith, W. P. and Kedward, K. T., Shear damage mechanisms in a woven, nicalon reinforced ceramic matrix composite. *J. Am. Ceram. Soc.*, 1997, **80**(2), 357–364.
11. Cooper, R. F. and Hall, P. C., Reactions between synthetic mica and simple oxide compounds with application to oxidation-resistant ceramic composite. *J. Am. Ceram. Soc.*, 1993, **76**(5), 1265–1273.
12. Morgan, P. E. D. and Marshall, D. B., Functional interfaces in oxide–oxide composites. *J. Mat. Sci. Eng.*, 1993, **A162**(1–2), 15–25.
13. Cinibulk, M. K., Magnetoplumbite compounds as a fiber coating for oxide–oxide composites. *Ceram. Eng. and Sci. Proc.*, 1994, **15**(5), 721–728.
14. Petuskey, W.T. (private communication).
15. Morgan, P. E. D. and Marshall, D. B., Ceramic composites of monazite and alumina. *J. Am. Ceram. Soc*, 1995, **78**(6), 1553–1563.
16. Morgan, P. E. D., Marshall, D. B. and Housley, R. M., High temperature stability of monazite-alumina composites. *J. Mat. Sci. Eng.*, 1995, **A195**, 215–222.
17. Marshall, D. B., Morgan, P. E. D. and Housley, R. M., Debonding in multilayered composites of zirconia and $LaPO_4$. *J. Am. Ceram. Soc.*, 1997, **80**(7), 1677–1683.
18. Marshall, D. B., Morgan, P. E. D., Housley, R. M. and Cheung, J. T., High temperature stability of the Al_2O_3-$LaPO_4$ system. *J. Am. Ceram Soc.*, 1998, **81**(4), 951–956.

19. Kuo, D.-H. and Kriven, W. M., Characterization of yttrium phosphate and a yttrium phosphate/yttrium aluminate laminate. *J. Am. Ceram. Soc*., 1995, **78**(11), 3121–3124.
20. Goettler, R. W., Sambasivan, S. and Dravid, V. P., Isotropic complex oxides as fiber coatings for oxide–oxide CFCC. *Ceramic Engineering and Science Proceedings*, 1997, **18**, 279–286.
21. Cain, M. G., Cain, R. L., Tye, A., Rian, P., Lewis, M. H. and Gent, J., Structure and stability of synthetic interphases in CMCs. *Key Engineering Materials*, 1997, **127–131**, 37–49.
22. Kerans, R. J., The role of coating compliance and fiber/matrix interfacial topography on debonding in ceramic composites. *Scripta Metall Mater*, 1995, **32**, 505–509.